UNIVERSITY OF CALIFORNIA SAN DIEGO

Y-Box Binding Proteins Regulate $CD8^+$ T Cell Differentiation and Function

A Thesis submitted in partial satisfaction of the requirements for the degree, Master of Science

in

Biology

by

Max Tyler Mamroth

Committee in Charge:

Professor John Chang, Chair
Professor Ananda Goldrath, Co-Chair
Professor Elina Zuniga

2019

The Thesis of Max Mamroth is approved, and it is acceptable in quality and form for publication on microfilm and electronically:

_____

_____

Co-Chair

_____

Chair

University of California San Diego

2019

TABLE OF CONTENTS

List of Figures

ABSTRACT OF THE THESIS

Y-Box Binding Proteins Regulate $CD8^+$ T Cell Differentiation and Function

by

Max Tyler Mamroth

Master of Science in Biology

University of California San Diego, 2019

Professor John Chang, Chair
Professor Ananda Goldrath, Co-chair

$CD8^+$ T cells are important for pathogen clearance and have many intrinsic and extrinsic factors that can determine how they differentiate into effector and memory cells. The Y-box binding protein (YBX) family of genes have been identified as potential regulators of $CD8^+$ T cell differentiation as early as the first division (Kakaradov et al. 2017). Previous studies have shown that YBX1 and YBX3 affect various cellular pathways and functions; however, none have focused on YBX genes affecting $CD8^+$ T cell differentiation and function. To address this gap in knowledge, this thesis investigated the effects on $CD8^+$ T cell differentiation at early and late time points in an acute infection model using an shRNA approach. To do this, we validated

retroviral shRNAs that knocked down YBX1 and YBX3, and a control non-targeting retroviral construct. Activated P14 CD45.1 and CD45.1.2 $CD8^+$ T cells were transduced with targeting and non-targeting retroviruses, respectively, and adoptively transferred into recipient mice that weresubsequently infected with lymphocytic choriomeningitis virus (LCMV) Armstrong. Seven days and thirty days after infection, mice were sacrificed, and spleen and small intestine tissue were analyzed using flow cytometry. Relative to the non-targeting control-transduced cells, cells knocked down for YBX1 and YBX3 expression exhibited reduced $CD8^+$ TE and $CD8^+$ T_{CM} populations. Knockdown of YBX1 and YBX3 expression also resulted in an increase of $CD8^+$ T_{RM} cells within the small intestine, and an increase of circulating T_{EM} cells and cytokine-producing cells.

Introduction

Cytotoxic T cells ($CD8^+$ T cells) are a type of adaptive immune cell important for pathogen clearance (Bender B., Croghan T., Zhang L. Small P., 1992), and have been shown to differentiate into both terminal effector (TE cells) cells and different memory cell subsets in response to infection (Gerlach et al., 2007, Kaech and Wherry, 2007, Chang, Wherry, and Goldrath, 2014). $CD8^+$ TE cells express killer cell lectin-like receptor G1 (KLRG1) at high levels and IL-7R at low levels ($KLRG1^{hi}IL\text{-}7R^{lo}$); this subset appears early after acute infection, is terminally differentiated, and has lost its ability to proliferate further, but can still produce cytokines necessary to fight infection such as interferon gamma (IFN-γ) or tumor necrosis factor alpha (TNF-α) (Joshi et al. 2007, Kaech et al., 2003, Hamann et al., 1997). Memory precursor (MP) cells ($KLRG1^{lo}IL\text{-}7R^{hi}$) do not give rise to only one memory cell subset, but depending on various signals, can differentiate into various types of memory cells (Kaech et al., 2003, Sallusto F., Lening D., Forester R., Lipp M., and Lanzavecchia A., 1999, Casey et al., 2012, Harty and Badovinac, 2008). One such subset, tissue-resident memory (T_{RM}) cells, express surface markers CD69 and CD103 (Kumar et al., 2017, Sathaliyawa et al., 2013) and are commonly located at mucosal sites where microbes are most often encountered such as the intraepithelial lymphocytes (IEL) (Schenkel J. and Masopust D., 2014, Sheridan and Lefrancois, 2010). Two long-lived circulating memory $CD8^+$ T cell subtypes are effector memory (T_{EM}) and central memory (T_{CM}) T cells. T_{CM} cells express high levels of CD62L and IL-7R ($CD62L^{hi}IL\text{-}7R^{hi}$), are lymph-node homing but lack inflammatory and cytotoxic function, and can differentiate to T_{EM} cells; T_{EM} cells lack CD62L but still express high levels of IL-7R ($CD62L^{lo}IL\text{-}7R^{hi}$), are tissue-homing, and can mediate inflammatory reactions and cytotoxicity (Sallusto F. et al., 1999, Faassen et al., 2005, Huster et al., 2004). $CD8^+$ T_{RM} cells and effector T cells produce cytokines such as IFN-γ, TNF-α, or interleukin 2 (IL-2) to cause inflammation or promote expansion of immune cells during an infection (Seder et al., 2008, Kumar et al., 2017).

Prior studies have shown that transcription factors, such as T-bet, and the amount of inflammation present, as indicated by inflammatory cytokines such as IFN-γ or TNF-α, play a pivotal role in early $CD8^+$ T cell differentiation (Joshi et al., 2007, Badovinac et al., 2004). One gene that has been identified

as a potential regulator of $CD8^+$ T cell differentiation at the first division for differentiation of TE cells is the Y-box binding protein (YBX) family of genes (Kakaradov et al., 2017). YBX1 and YBX3, both cold shock domain proteins, located on human chromosome 1 and 12 respectively, are known to have regulatory effects on cell differentiation, cell trafficking, cellular proliferation, and cytokine synthesis in a variety of inflammatory diseases and cancers (Bernhardt et al., 2017 Lovett et al., 2010, Bergmann et al., 2005, Linquist et al., 2014). Because no studies have investigated the effects YBX1 or YBX3 have on regulating $CD8^+$ T cells differentiation in an acute infection model, we generated retroviruses encoding short hairpin RNA (shRNA) that knockdown YBX1 or YBX3 to transduce into $CD8^+$ T cells. We then studied how knockdown of YBX1 and YBX3 affected $CD8^+$ T cells differentiation into effector and memory subsets *in vivo* after exposure to lymphocytic choriomeningitis virus (LCMV) Armstrong. We hypothesized that YBX1 and YBX3 would have a pivotal role on differentiation of $CD8^+$ TE and MP cells, as well as exhibit a continued effect through differentiation into memory cells.

Methods and Materials

Mice

All mice were housed in specific pathogen-free conditions. All experiments were approved and conducted in accordance with the Institutional Animal Care and Use Committees (IACUC) of the University of California, San Diego. Wild type C57BL/6J mice were purchased from Jackson Laboratory. LCMV GP 33-41 TCR-transgenic P14 mice and mice with expression of congenic molecules CD45.1, CD45.1.2, or CD45.2 were maintained in our colony.

Isolations

For isolation of small intestine intraepithelial lymphocytes (IEL), the small intestine was removed, Peyer's patches were excised, and the intestine was cut longitudinally and then cut laterally into $1cm^2$ pieces. These pieces were incubated in 10% HBSS/HEPES bicarbonate with 0.154 mg/mL dithioerythritol (DTE) for 30 minutes at 37°C while stirred at 200 RPM. From the supernatant, lymphocytes were separated using a 44/67% Percoll (Sigma Aldrich) density gradient. Spleens were mechanically dissociated, filtered through a 70μm nylon cell strainer (Falcon), and treated with a red blood cell lysis buffer (Sigma Aldrich).

Antibodies, intracellular staining, flow cytometry, and cell sorting

Flow cytometry analysis was performed on a BD AccuriC6 or BD LSRFortessa X-20. Cell sorting was performed on BD FACSAria. The following antibodies were used: anti-CD8α (clone 53-6.7), anti-KLRG1 (2F1), anti-CD45.1 (A20), anti-CD45.2 (104), anti-IL-7R (A7R34), anti-CD69 (FN50), anti-CD43-A (1B11), anti-CD62L(MEL-14), anti-CD103 (2E7), anti-CX3CR1 (SA011F11), anti-CD27 (LG.3A10), anti-IFN-γ (XMG1.2), anti-TNF-α (MP6-XT22),

anti-IL-2 (JES6-5H4), anti-Tbet (4B10), anti-KI67 (Ki-67; all from Biolegend), and anti-Foxo1(C29H4), anti-TCF7 (C63D9, both from Cell Signaling Technology). To analyze cytokine production, $CD8^+$ T cells were re-stimulated with the gp33-41 peptide for 3 or 4 hours for IEL or splenic tissue respectively. For intracellular staining of cytokines or transcription factors while preserving Ametrine expression, cells were fixed with 2% PFA diluted in PBS for 45 minutes in the dark at room temperature. Intracellular staining for cytokines was performed using Permeabilization Buffer 10X purchased from Invitrogen. Transcription factor staining was performed using Permeabilization Buffer 10X purchased from eBioscience.

shRNA development and validation of knockdown using qPCR

YBX1 and YBX3 knockdown construct plasmids were isolated from bacterial colonies obtained from transOMIC technologies using a maxiprep kit (Qiagen) and concentration measured using a NanoDrop spectrometer (Thermo Scientific). The vectors were then frozen at -20℃ until needed. For transfections, 293T cells were plated on 100mm × 30mm plates (Falcon) at a density of 9×10^6 cells per plate one day prior to transfection. Each plate was then transfected with 30µg of target DNA and 15µg of pCL-Eco. Retroviral supernatant was harvested at 32 hours and 56 hours after transfection.

For $CD8^+$ T cell activation *in vitro*, naïve $CD8^+$ T cells from spleen and lymph nodes were negatively enriched using a $CD8^+$ T cell isolation kit II (Miltenyi Biotec) and 1×10^6 $CD8^+$ T cells were plated in the middle 24 wells of a 48-well plate that were pre-coated with 100µg/mL goat anti-hamster IgG (H+L, Invitrogen) and 5µg/mL anti-CD3 and 5µg anti-CD28. 18 hours after activation, media was removed and replaced with retroviral supernatant with 10mg/ml polybrene (Millipore/Fisher) followed by spinfection (90 min. centrifugation at 950 × g). 1 hour

after spinfection, the $CD8^+$ T cells were washed, and media was replaced with full media and 10U/mL of IL-2. 72 hours after media was replaced, 90% of each construct's wells were pooled together, washed with HBSS containing 1% FBS and sorted by CD8 and Ametrine positivity using BD FACSAria. Cells were then stored in QIAzol (Qiagen) reagent and frozen in $-80^{O}C$ until needed. RNA was extracted from these cells using the RNeasy mini kit by Qiagen. Equal amounts of RNA were used to synthesize cDNA using the cDNA synthesis kit by Applied Biosystems. Primers were designed using Primer-BLAST. Quantitative PCR was performed on a CFX96 qPCR machine (Bio-Rad) using SsoAdvanced SYBRgreen Supermix (Bio-Rad). The ΔΔCt method was used to calculate relative levels of gene expression; RPL13 was used as a normalization control. The sequences for primers used in this study: YBX1 forward 5'-GCCGGCTTACCATCTCTACC -3', and YBX1 reveres 5'- GAAACACCCCAGACTAGCCC -3'. YBX3 forward 5'-AAAGAGACCAAGGCAGGTGA-3', and YBX3 reverse 5'-GTAAGGTCGTGGGTGTGCTT-3'.

$CD8^+$ T cell transduction, cell transfer, and infection

Naïve $CD8^+$ T cells were isolated and transduced with shRNAs as described above, washed and transferred into mice within 6 hours after spinfection. Recipient congenic CD45.2 mice were injected intravenously with a 1:1 ratio of sex-matched $P14^+$ $CD8^+$ T cells. CD45.1 and CD45.1.2 cells were transduced with either target or non-targeting retrovirus, respectively. A total of 1.5×10^5 transduced P14 $CD8^+$ T cells were injected into each recipient. One hour after transfer, recipient mice were infected through intraperitoneal (i.p) injection with 2×10^5 PFU lymphocytic choriomeningitis virus (LCMV) Armstrong. All experiments were performed either seven days or thirty days after infection with LCMV Armstrong.

Statistics

Data was analyzed using a paired parametric students t-test; differences at *p* values less than .05 were considered significant. Statistical analyses were performed using Prism 7 (GraphPad Software Inc, San Diego, CA, USA).

Results

Validation of Knockdown for YBX1 and YBX3

To determine knockdown efficiency, we transduced naïve $CD8^+$ T cells with Ametrine-expressing retroviruses expressing short hairpin RNA (shRNA) targeting YBX1 (shYBX1) or YBX3 (shYBX3), or a nontargeting control (shControl). After 72 hours the transduced cells were FACS sorted by Ametrine-positive $CD8^+$ T cells, and RNA was extracted from 3×10^5 transduced $CD8^+$ T cells. Equal amounts of RNA were synthesized into cDNA and measured using Quantitative Real-Time PCR to determine percent expression changes (**Fig. 1A**). Relative to control cells transduced with shControl, knockdown of YBX1 resulted in a 93.5% reduction of its expression (**Fig. 1B**), and knockdown of YBX3 resulted in a 93% reduction of expression (**Fig. 1C**).

Knockdown of YBX3 results in a reduction of $CD8^+$ TE cells and an increase of $CD8^+$ MP cells, small intestine $CD8^+$ T_{RM} cells, and cytokine-producing cells in spleen and IEL

To investigate the effects on $CD8^+$ T cells transduced with shYBX3, activated P14 $CD8^+$ T cells expressing the congenic marker CD45.1 were transduced with the shYBX3 retrovirus, while activated P14 $CD8^+$ T cells expressing the congenic marker CD45.1.2 were transduced with the shControl retrovirus. A 1:1 mixture of these cells were injected i.v. into recipient CD45.2 mice, followed by i.p. infection of recipient mice with LCMV Armstrong one hour later (**Fig. 2A**). To determine how YBX3 regulates circulating $CD8^+$ T cells, recipient mice were sacrificed and splenocytes were analyzed on day seven post-infection by flow cytometry. Knockdown of YBX3 resulted in a significantly reduced number and frequency of $KLRG1^{hi}IL\text{-}7R^{lo}$ TE phenotype cells (**Fig. 2B, 2C**). By contrast, knockdown of YBX3 resulted in

significantly reduced numbers and frequencies of KLRG1^{lo}IL-7R^{hi} MP phenotype cells (**Fig. 2D**). Next, we evaluated whether knockdown of YBX3 would alter the production of inflammatory cytokines by circulating CD8$^+$ T cells. CD8$^+$ T cells from the spleens of recipient mice were restimulated with gp33-41 protein for 4 hours and then analyzed with flow cytometry. Knockdown of YBX3 resulted in increased numbers and frequencies of CD8$^+$ T cells expressing IFN-γ, TNF-α, and IL-2 (**Fig. 2E-G**). Moreover, the mean fluorescence intensity of TNF-α in cells knocked down for YBX3 was increased when compared to cells transduced with shControl (**Fig. 2H**).

Lastly, we sought to assess the role of YBX3 in the differentiation of small intestine IEL T_{RM} CD8$^+$ T cells. Seven days after infection of recipient mice with LCMV Armstrong, flow cytometry of IEL revealed that compared to shControl, knockdown of YBX resulted in increased numbers of CD8$^+$ CD69$^+$ CD103$^+$ cells (**Fig. 2I, 2J**). Knockdown of YBX3 also resulted in increased numbers and frequencies of small intestine CD8$^+$ T cells producing IFN-γ, TNF-α, and IL-2 (**Fig. 2K-M**). Moreover, the mean fluorescence intensities of TNF-α and IFN-γ were increased in cells transduced with shYBX3 compared to shControl transduced cells (**Fig. 2N**).

YBX3 regulates CD8$^+$ T_{EM} cell differentiation and small intestine T_{RM} cell cytokine production 30 days after infection

To determine the effects of YBX3 on memory cell differentiation, splenocytes and IEL were isolated from recipient mice 30 days after infection with LCMV Armstrong. Measuring CD62L and IL-7R of CD8$^+$ T cells from splenocytes using flow cytometry indicated a substantial increase in number and frequency of the T_{EM} cell subset (CD62L^{lo} IL-7R^{hi}) in cells transduced with shYBX3 relative to cells transduced with shControl (**Fig. 3A-C**). Furthermore, we observed

a reduction in the numbers and frequencies of the long-lived effector T cell (LLE, CD62L^{lo}IL-7R^{lo}) and T_{CM} cell (CD62L^{hi}IL-7R^{hi}) subsets, relative to CD8$^+$ T cells transduced with shControl (**Fig. 3A-C**). However, at 30 days post-infection, splenic CD8$^+$ T cells transduced with shYBX3 or shControl were not different in their ability to produce IFN-γ, TNF-α, or IL-2 (**Fig. 3D-G**).

Consistent with our observations in the small intestines of recipient mice seven days after infection, YBX3 knockdown resulted in reduced numbers and frequencies of CD8$^+$ CD69$^+$ CD103$^+$ cells 30 days after infection (**Fig. 3H, 3I**). However, these cells exhibited an increased propensity to produce IFN-γ, TNF-α, and IL-2 30 days after infection (**Fig. 3J-L**). The mean fluorescence intensities of IFN-γ, TNF-α, and IL-2 were not different in cells transduced with shYBX3 compared to those transduced with shControl (**Fig. 3M**).

Knockdown of YBX1 affects circulatory and IEL effector CD8$^+$ T cell differentiation and function

Using an identical approach as that used to study YBX3, CD45.1 or CD45.1.2 P14 CD8$^+$ T cells were transduced with retrovirus encoding shRNA targeting YBX1 or a non-target control retrovirus, respectively. Cells were injected i.v. into recipient mice which were subsequently infected with LCMV Armstrong (**Fig. 2A**). Seven days after infection, spleens and small intestine IEL were harvested from recipient mice and analyzed by flow cytometry. Consistent with knockdown of YBX3, knockdown of YBX1 resulted in a significantly reduced number and frequency of TE phenotype cells relative to cells transduced with shControl (**Fig. 4A, 4B**). Knockdown of YBX1 resulted in a significant increase of frequency of MP phenotype cells; however, compared to shControl, knockdown of YBX1 did not result in a greater absolute number of MP cells (**Fig. 4A, 4C**).

To investigate the role YBX1 has on cytokine production seven days after infection, $CD8^+$ T cells from the spleens of recipient mice were restimulated with gp33-41 peptide for 4 hours and analyzed with flow cytometry. Compared to shControl, when YBX1 was knocked down, $CD8^+$ T cells exhibited a reduction in number, but an increase in frequency of IFN-γ and TNF-α-producing cells (**Fig. 4D, 4E**); however, there was no difference in frequency of IL-2-producing cells seven days after infection (**Fig. 4D, 4F**). Interestingly, a decrease in mean fluorescence intensity of IFN-γ was observed in cells knocked down for YBX1 relative to those transduced with shControl (**Fig. 4G)**. Lastly, seven days after infection, small intestine IEL $CD8^+$ $CD69^+$ $CD103^+$ cells knocked down for YBX1 were increased in frequency compared to cells transduced with shControl; moreover, the number of cells were significantly reduced (**Fig. 4H, 4I**).

YBX1 regulates $CD8^+$ T_{EM} cell and small intestine $CD8^+$ T_{RM} cell differentiation and function

At 30 days after infection with LCMV Armstrong, YBX1 knockdown resulted in decreased numbers of LLE, T_{EM}, and T_{CM} memory subsets (**Fig. 5A, 5B**). Like cells knocked down for YBX3, cells that were knocked down for YBX1 were observed to have an increase in the frequency of T_{EM} cells, and decreased frequency of LLE cells and T_{CM} cells (**Fig. 5C**). At 30 days post-infection, knockdown of YBX1 resulted in no differences in number, frequency, or mean fluorescence intensities of IFN-γ and TNF-α-producing cells compared to control (**Fig. 5D, 5E**). However, these cells exhibited a reduction in frequency of IL-2 producing cells, although the absolute numbers and MFI of these cells were unchanged (**Fig. 5D, 5F, 5G**). Lastly,

knockdown of YBX1 resulted in an increased frequency but decreased absolute number of small intestine $CD8^+$ $CD69^+$ $CD103^+$ cells 30 days after infection (**Fig. 5H, 5I**).

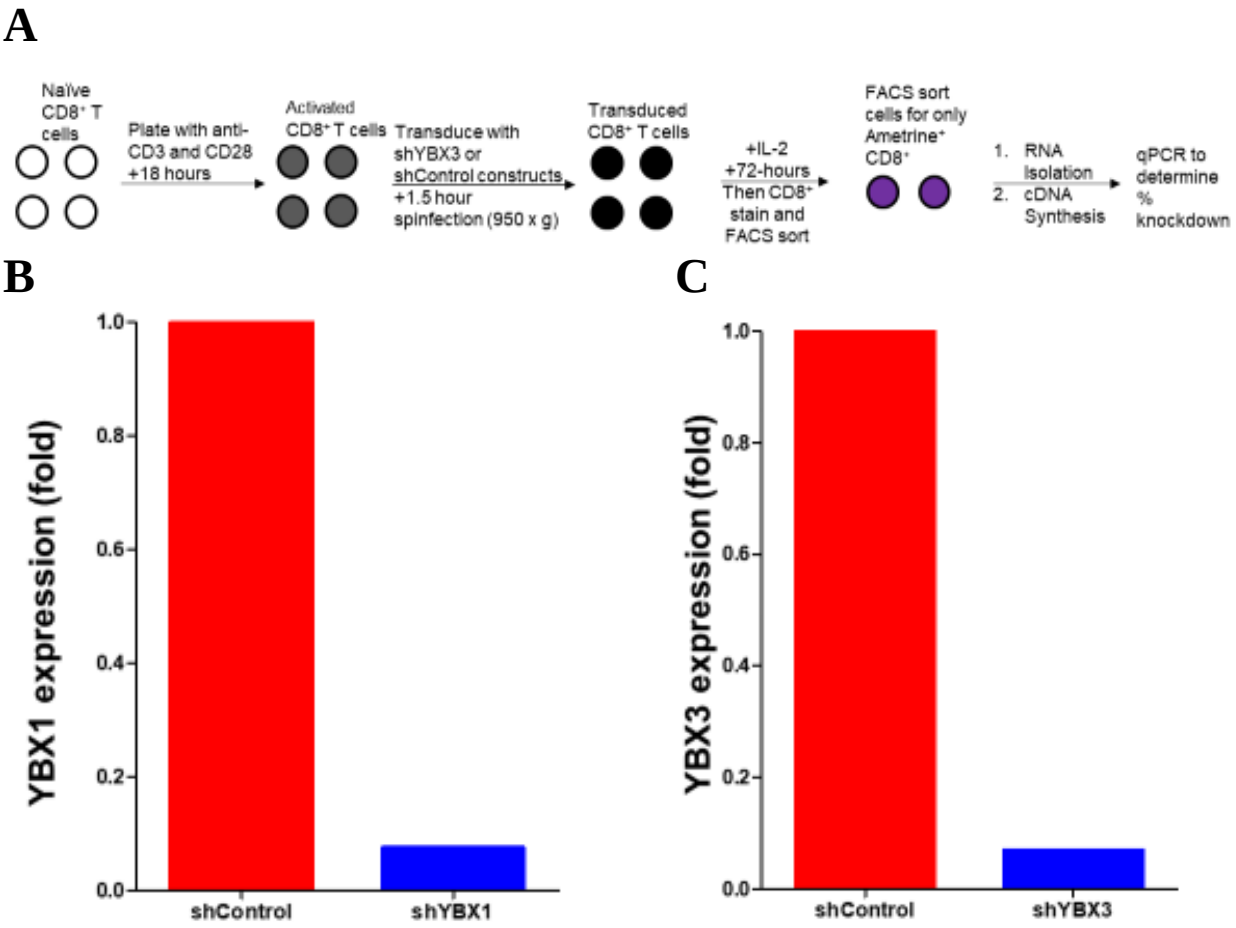

Figure 1: Validation of retrovirus to knockdown specific genes. **(A)** Naïve $CD8^+$ T cells were isolated from C57BL/6 mice and activated *in vitro* using anti-CD3 and anti-CD28 mAbs. After 18 hours activated cells were transduced via spinfection with retrovirus targeting YBX3, or YBX1, or a nontargeting control construct. Following spinfection, IL-2 was added to media for 72 hours. Transduced cells were then stained with anti-CD8 antibody and FACS sorted for $Ametrine^+$ $CD8^+$ T cells. Following cell sorting, 3 x 10^5 cells were used for RNA extraction. Equal amounts of RNA were then used for cDNA synthesis. Finally, qPCR was performed using equal amounts of cDNA. **(B)** qPCR analysis of YBX1 mRNA; results are presented relative to those of shControl-transduced cells. **(C)** qPCR analysis of YBX3 mRNA; results are presented relative to those of shControl-transduced cells.

Figure 2: YBX3 regulates circulating effector $CD8^+$ T cell differentiation, IEL $CD8^+$ T_{RM} differentiation, and T cell function. **(A)** Naïve $CD8^+$ T cells were isolated from CD45.1 or CD45.1.2 P14 mice and activated *in vitro* using anti-CD3 and anti-CD28 mAbs. After 18 hours, activated cells were transduced via spinfection with retrovirus targeting YBX3 (onto CD45.1 P14 $CD8^+$ T cells) or a nontargeting control construct (CD45.1.2 P14 $CD8^+$ T cells). Within 6 hours of spinfection, transduced cells were counted and mixed into a 1:1 ratio of transduced CD45.1 cells to CD45.1.2 cells. 200µl of cells totaling $1.5x10^5$ transduced cells were then injected intravenously (i.v.) into recipient mice. 1 hour after transfer of cells, recipient mice were infected intraperitoneally (i.p.) with $2x10^5$ PFU of Lymphocytic choriomeningitis virus (LCMV) Armstrong. **(B)** Flow cytometry of shRNA-transduced cells from host mice following i.v. co-transfer of P14 $CD8^+$ T cells that had been activated *in vitro* and transduced for 6h with shControl or shYBX3 constructs, followed by i.p. infection of the recipients with LCMV Armstrong (as in **2A**). Splenocytes were analyzed seven days later for KLRG1 and IL-7R expression. Numbers in quadrants indicate percent cells. Plot on the right indicates gating strategy for TE and MP subsets. **(C)** Quantification (left) or frequency (right) of TE $CD8^+$ T cells as in **B**. **(D)** Quantification (left) or frequency (right) of MP $CD8^+$ T cells as in **B**. **(E)** Flow cytometry of splenocytes was performed as described in **B** and analysis of TNF-α, IFN-γ, and IL-2 expression is shown. Cells were stimulated for 4 hours with gp33 peptide. Numbers in quadrants indicate percent cells. **(F)** Quantification (left) or frequency (right) of splenic TNF-α^+ IFN-γ^+ $CD8^+$ T cells as in **E**. **(G)** Quantification (left) or frequency (right) of splenic IL-2^+ $CD8^+$ T cells as in **E. (H)** Mean fluorescent intensity (MFI) of splenic TNF-α^+ (left), IFN-γ^+ (middle), or IL-2^+ (right) $CD8^+$ T cells as in **E**. **(I)** Flow cytometry of cells as described in **B**. Intraepithelial lymphocytes (IEL) isolated from the small intestinal tissue were analyzed seven days later and CD69 and CD103 expression was quantified. Numbers in quadrants indicate percent cells. **(J)** Quantification (left) or frequency (right) of IEL $CD8^+$ $CD69^+$ $CD103^+$ cells as in **I**. **(K)** Flow cytometry of IEL isolated from the small intestinal tissue performed as described in **I** and analysis of TNF-α, IFN-γ, and IL-2 expression is shown. Cells were stimulated with gp33 peptide for 3 hours. Numbers in quadrants indicate percent cells. **(L)** Quantification (left) or frequency (right) of IEL TNF-α^+ IFN-γ^+ $CD8^+$ T cells as in **K**. **(M)** Quantification (left) or frequency (right) of IEL IL-2^+ $CD8^+$ T cells as in **K**. **(N)** MFI of IEL TNF-α^+ (left), IFN-γ^+ (middle), and IL-2^+ (right) $CD8^+$ T cells as in **K**. n = 4 for all groups. Data reported as mean +/- SEM.* P < .05, ** P <.01, *** P < .001, **** P <.0001 (paired parametric t-test). Data are representative of two experiments.

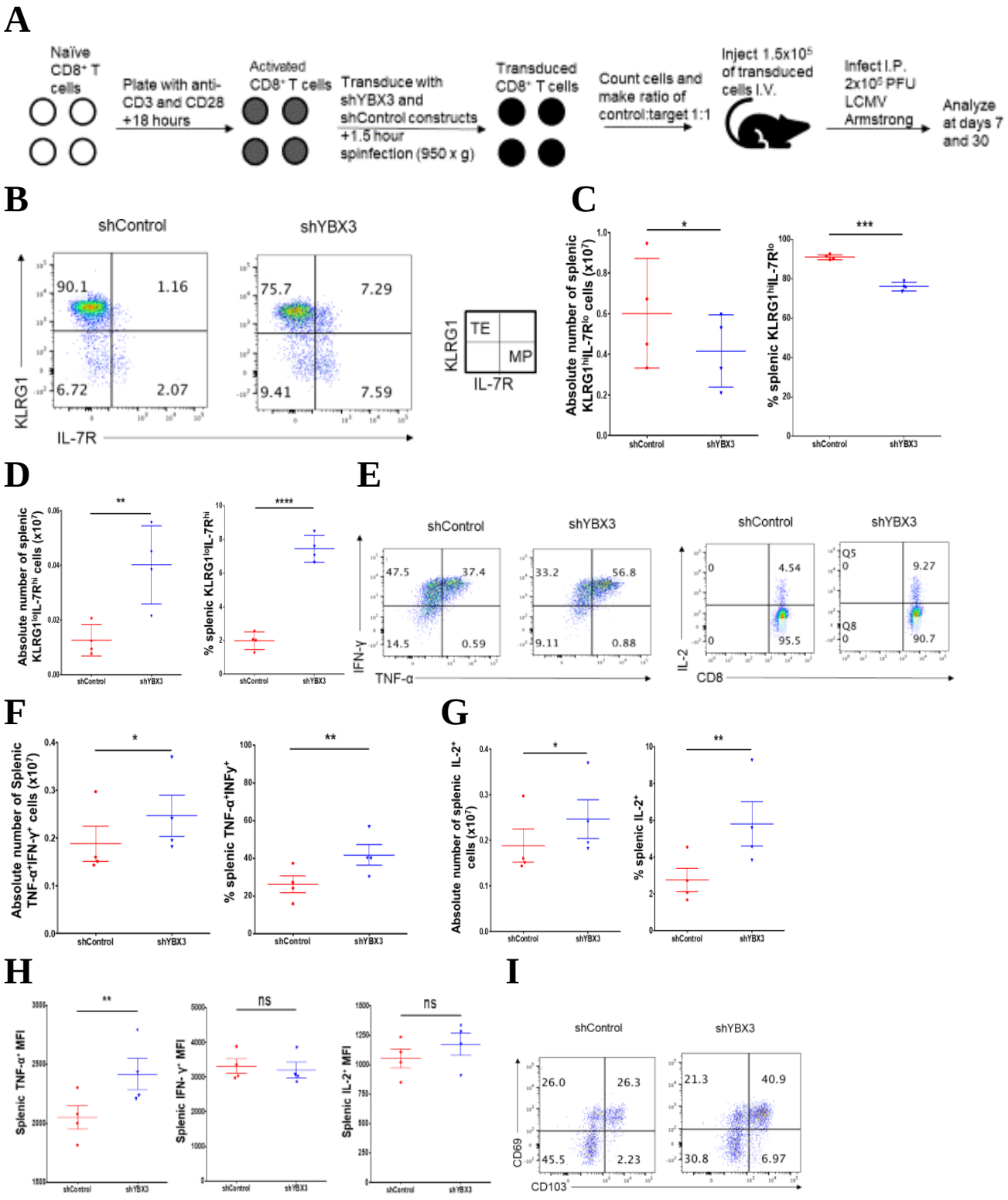
A
Naïve CD8+ T cells
Plate with anti-CD3 and CD28 +18 hours
Activated CD8+ T cells
Transduce with shYBX3 and shControl constructs +1.5 hour spinfection (950 x g)
Transduced CD8+ T cells
Count cells and make ratio of control:target 1:1
Inject 1.5x10^5 of transduced cells I.V.
Infect I.P. 2x10^5 PFU LCMV Armstrong
Analyze at days 7 and 30
B
shControl
shYBX3
90.1
1.16
6.72
2.07
75.7
7.29
9.41
7.59
KLRG1
IL-7R
TE
MP
C
Absolute number of splenic KLRG1hiIL-7RIo cells (x10^7)
% splenic KLRG1hiIL-7RIo
shControl
shYBX3
D
Absolute number of splenic KLRG1IoIL-7Rhi cells (x10^7)
% splenic KLRG1IoIL-7Rhi
E
shControl
shYBX3
47.5
37.4
14.5
0.59
33.2
56.8
9.11
0.88
IFN-γ
TNF-α
4.54
95.5
9.27
90.7
IL-2
CD8
F
Absolute number of Splenic TNF-α+IFN-γ+ cells (x10^7)
% splenic TNF-α+INFγ+
G
Absolute number of splenic IL-2+ cells (x10^7)
% splenic IL-2+
H
Splenic TNF-α+ MFI
Splenic IFN- γ+ MFI
Splenic IL-2+ MFI
ns
I
shControl
shYBX3
26.0
26.3
45.5
2.23
21.3
40.9
30.8
6.97
CD69
CD103

Figure 2 continued.

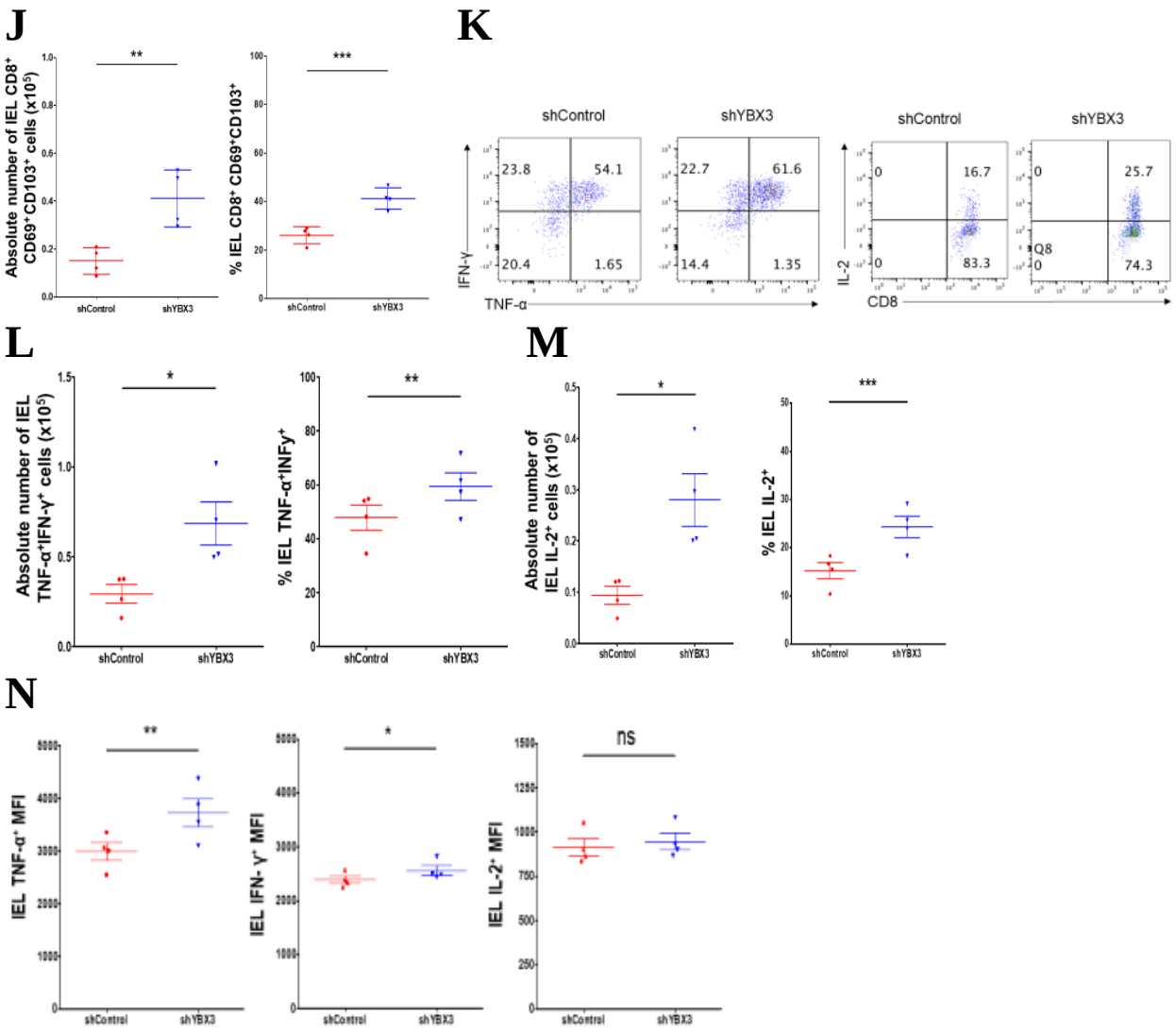

Figure 3: YBX3 regulates differentiation of circulating $CD8^+$ T_{EM} and T_{CM} cells, small intestine $CD8^+$ T_{RM} cells, and function of IEL $CD8^+$ T_{RM} cells. **(A)** Flow cytometry of shRNA-transduced cells from host mice following i.v. co-transfer of P14 $CD8^+$ T cells that had been activated *in vitro* and transduced for 6h with shControl or shYBX3, followed by i.p. infection of the hosts with LCMV Armstrong (as in **2A**). Splenocytes were analyzed 30 days later for CD62L and IL-7R expression. Numbers in quadrants indicate percent cells. Plot on the right indicates gating strategy for LLE, T_{EM}, and T_{CM} subsets. **(B)** Quantification of splenic LLE, T_{EM}, and T_{CM} $CD8^+$ T cells as in **A**. **(C)** Frequency of splenic LLE (left), T_{EM} (middle), and T_{CM} (right) $CD8^+$ T cells as in **A**. **(D)** Flow cytometry of splenocytes was performed as described in **A** and analysis of TNF-α, IFN-γ, and IL-2 expression is shown. Cells were stimulated for 4 hours with gp33 peptide. Numbers in quadrants indicate percent cells. **(E)** Quantification (left) or frequency (right) of splenic TNF-α^+ IFN-γ^+ $CD8^+$ T cells as in **D**. **(F)** Quantification (left) or frequency (right) of splenic IL-2^+ $CD8^+$ T cells as in **D**. **(G)** MFI of splenic TNF-α^+ (left), IFN-γ^+ (middle), and IL-2^+ (right) $CD8^+$ T cells as in **D**. **(H)** Flow cytometry of cells as described in **A**. IELs isolated from the small intestinal tissue were analyzed 30 days later and CD69 and CD103 expression was quantified. Numbers in quadrants indicate percent cells. **(I)** Quantification (left) or frequency (right) of IEL $CD8^+$ $CD69^+$ $CD103^+$ cells as in **H**. **(J)** Flow cytometry of IEL was performed as described in **H** and analysis of TNF-α, IFN-γ, and IL-2 expression is shown. Cells were stimulated with gp33 peptide for 3 hours. Numbers in quadrants indicate percent cells in each throughout. **(K)** Quantification (left) or frequency (right) of IEL TNF-α^+ IFN-γ^+ $CD8^+$ T cells as in **J**. **(L)** Quantification (left) or frequency (right) of IEL IL-2^+ $CD8^+$ T cells as in **J**. **(M)** MFI of IEL TNF-α^+ (right), IFN-γ^+ (middle), and IL-2^+ (right) cells $CD8^+$ T cells as in **J**. n = 4 for all groups. Data reported as mean +/- SEM. * $P < .05$, ** $P < .01$ (paired parametric t-test). Data are representative of two experiments.

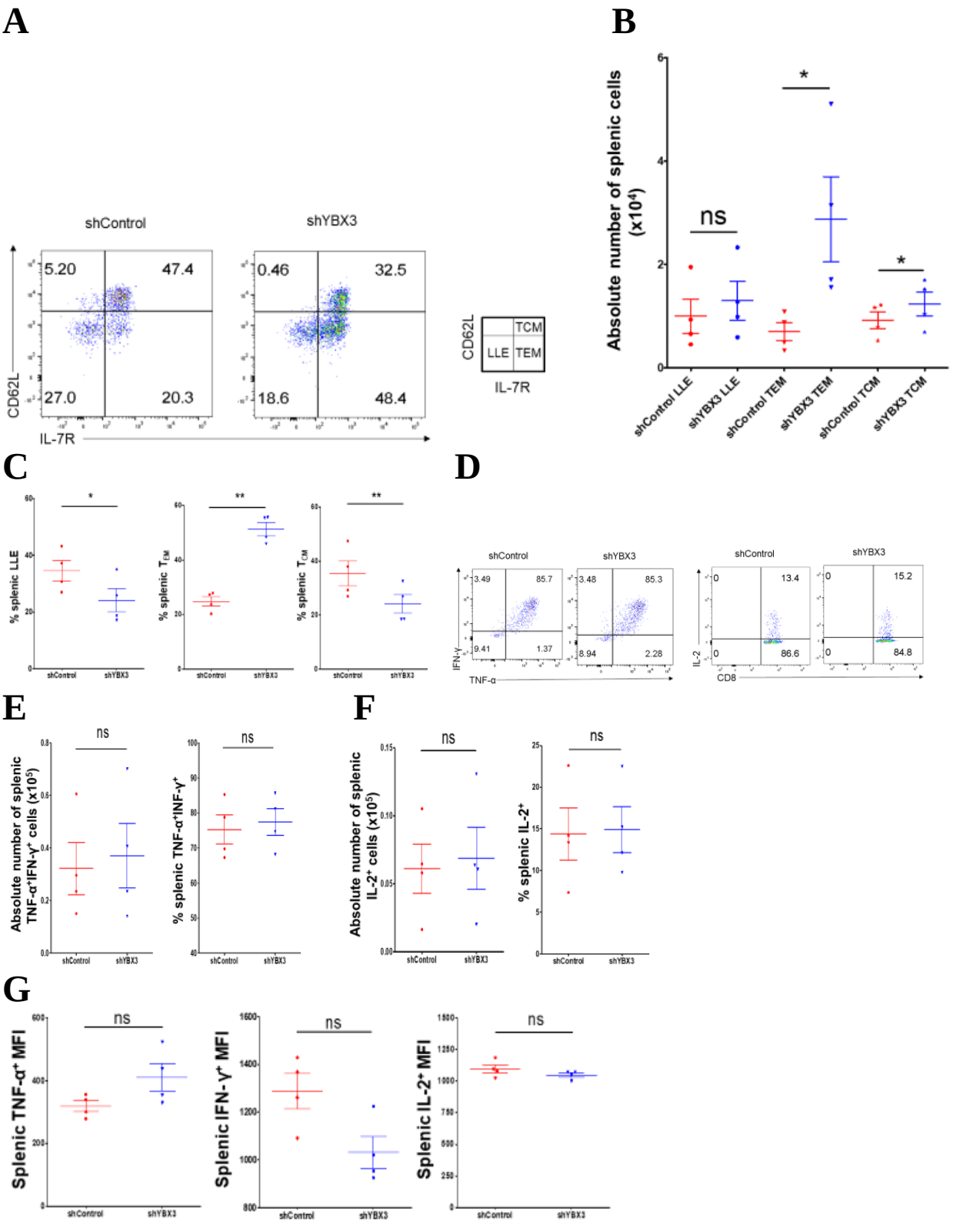
A
shControl
shYBX3
5.20
47.4
27.0
20.3
0.46
32.5
18.6
48.4
CD62L
IL-7R
LLE
TCM
TEM
B
Absolute number of splenic cells (x10⁴)
ns
*
*
shControl LLE
shYBX3 LLE
shControl TEM
shYBX3 TEM
shControl TCM
shYBX3 TCM
C
% splenic LLE
% splenic TEM
% splenic TCM
D
shControl
shYBX3
IFN-γ
TNF-α
IL-2
CD8
E
Absolute number of splenic TNF-α⁺IFN-γ⁺ cells (x10⁵)
% splenic TNF-α⁺INF-γ⁺
F
Absolute number of splenic IL-2⁺ cells (x10⁵)
% splenic IL-2⁺
G
Splenic TNF-α⁺ MFI
Splenic IFN-γ⁺ MFI
Splenic IL-2⁺ MFI

Figure 3 continued.

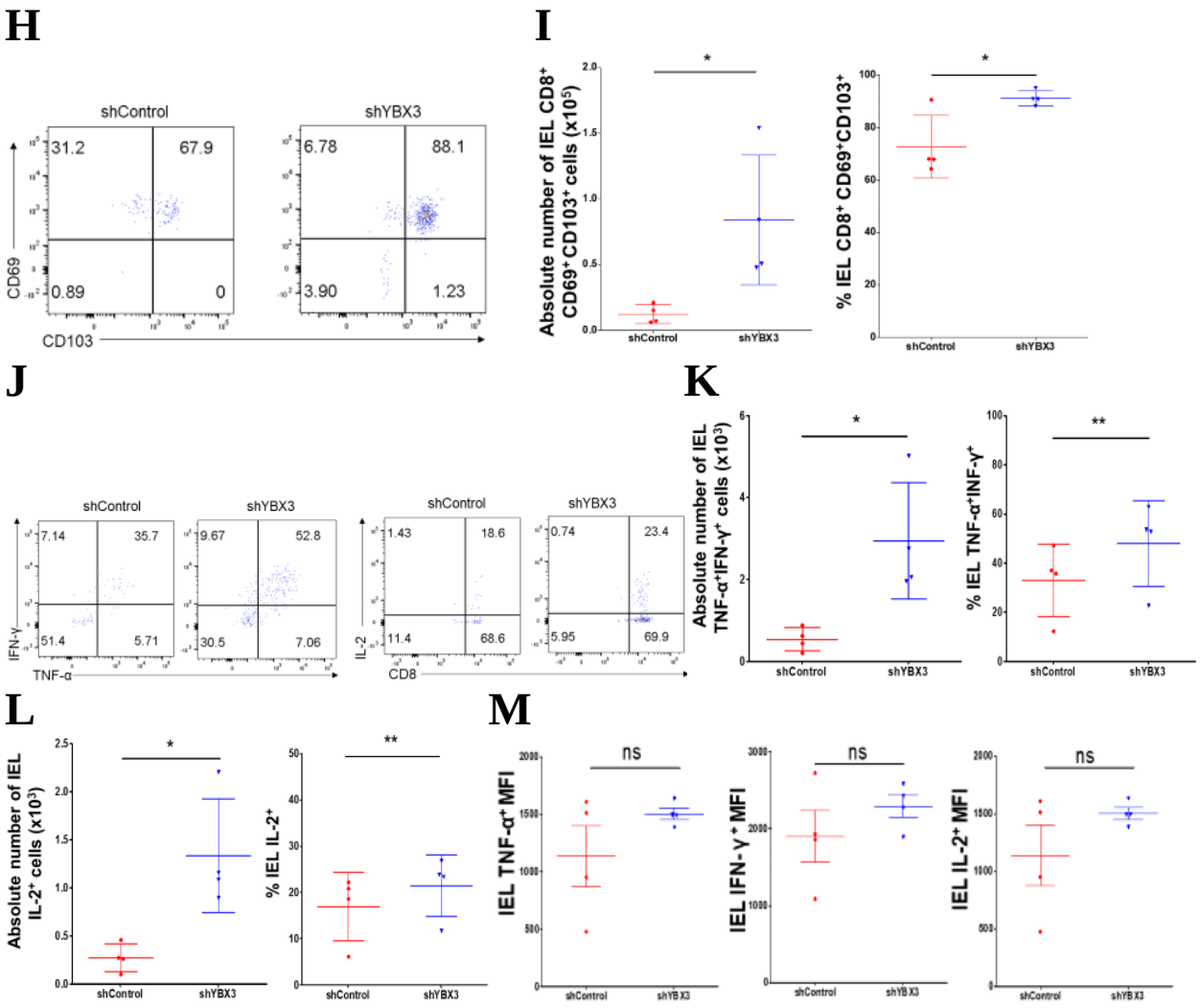

Figure 4: YBX1 regulates circulating effector $CD8^+$ T cell differentiation, IEL $CD8^+$ T_{RM} differentiation, and T cell function. **(A)** Flow cytometry of shRNA-transduced cells from host mice following i.v. co-transfer of P14 $CD8^+$ T cells that had been activated *in vitro* and transduced for 6h with shControl or shYBX1 constructs, followed by i.p. infection of recipient mice with Lymphocytic choriomeningitis virus (LCMV) Armstrong (as in **2A**). Splenocytes were analyzed seven days later for KLRG1 and IL-7R expression. Numbers in quadrants indicate percent cells. Plot on the right indicates gating strategy for TE and MP subsets. **(B)** Quantification (left) or frequency (right) of TE $CD8^+$ T cells as in **A**. **(C)** Quantification (left) or frequency (right) of MP $CD8^+$ T cells as in **A**. **(D)** Flow cytometry of splenocytes was performed seven days after infection as described in **A** and analysis of TNF-α, IFN-γ, and IL-2 expression is shown. Cells were stimulated for 4 hours with gp33 peptide. Numbers in quadrants indicate percent cells. **(E)** Quantification (left) or frequency (right) of splenic TNF-α^+ IFN-γ^+ $CD8^+$ T cells as in **D**. **(F)** Quantification (left) or frequency (right) of splenic IL-2^+ $CD8^+$ T cells as in **D.** **(G)** MFI of splenic TNF-α^+ (left), IFN-γ^+ (middle), or IL-2^+ (right) $CD8^+$ T cells as in **D**. **(H)** Flow cytometry of cells as described in **A**. IEL isolated from the small intestinal tissue were analyzed seven days later and CD69 and CD103 expression was quantified. Numbers in quadrants indicate percent cells. **(I)** Quantification (left) or frequency (right) of IEL $CD8^+$ $CD69^+$ $CD103^+$ cells as in **H**. n = 5 for all groups. Data reported as mean +/- SEM.* P < .05, ** P <.01, *** P < .001 (paired parametric t-test). Data are representative of four experiments.

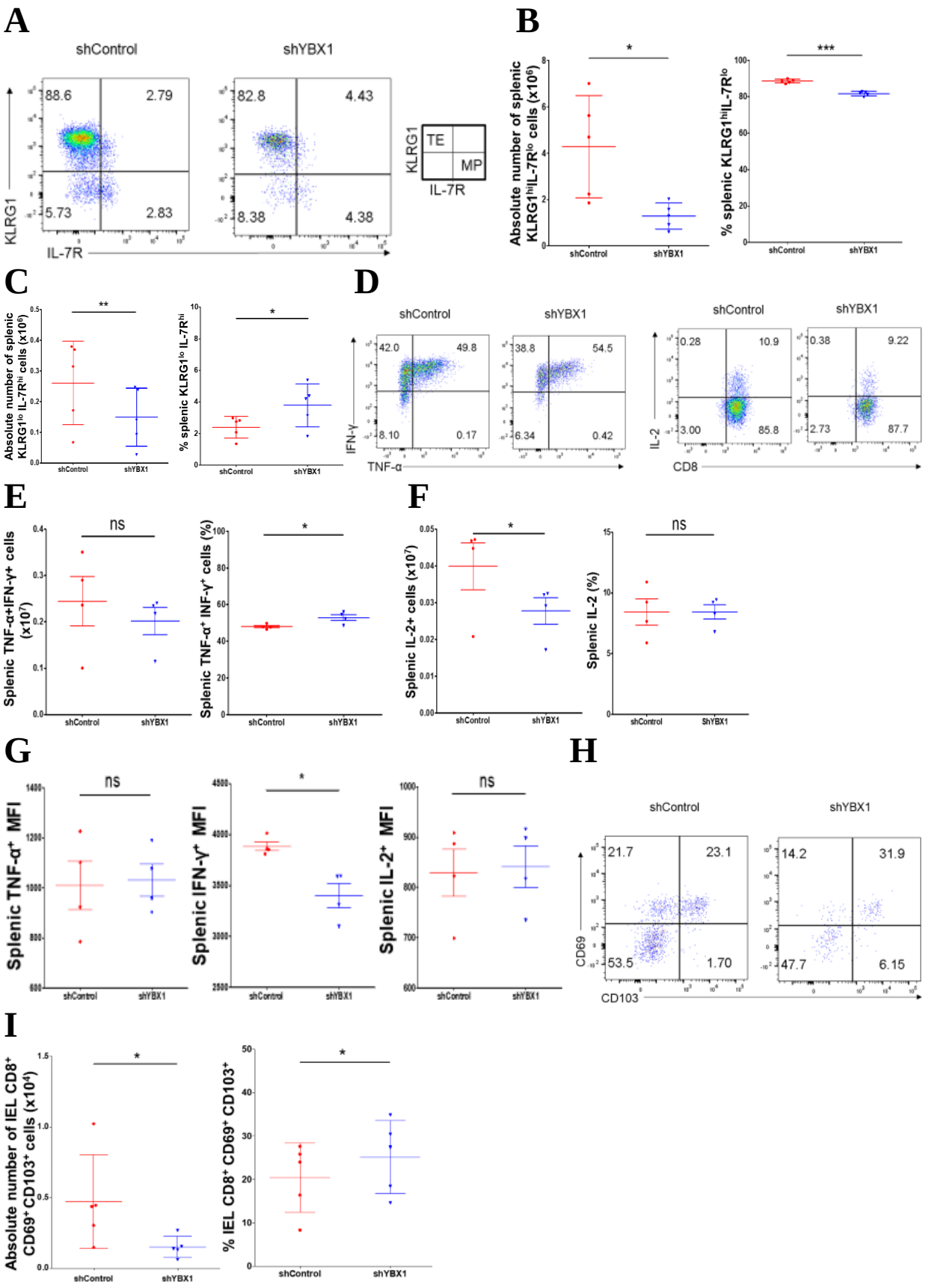
A
shControl
shYBX1
88.6
2.79
5.73
2.83
82.8
4.43
8.38
4.38
KLRG1
IL-7R
TE
MP
B
Absolute number of splenic KLRG1hiIL-7Rlo cells (x10⁶)
% splenic KLRG1hiIL-7Rlo
C
Absolute number of splenic KLRG1lo IL-7Rhi cells (x10⁶)
% splenic KLRG1lo IL-7Rhi
D
42.0
49.8
8.10
0.17
38.8
54.5
6.34
0.42
IFN-γ
TNF-α
0.28
10.9
3.00
85.8
0.38
9.22
2.73
87.7
IL-2
CD8
E
Splenic TNF-α+IFN-γ+ cells (x10⁷)
Splenic TNF-α+ INF-γ+ cells (%)
F
Splenic IL-2+ cells (x10⁷)
Splenic IL-2 (%)
G
Splenic TNF-α+ MFI
Splenic IFN-γ+ MFI
Splenic IL-2+ MFI
H
21.7
23.1
53.5
1.70
14.2
31.9
47.7
6.15
CD69
CD103
I
Absolute number of IEL CD8+ CD69+CD103+ cells (x10⁴)
% IEL CD8+ CD69+ CD103+
ns
*
**
***
shControl
shYBX1

Figure 5: YBX1 regulates differentiation of circulating $CD8^+$ T_{EM} and T_{CM} cells, small intestine $CD8^+$ T_{RM} cells, and T cell function. **(A)** Flow cytometry of shRNA-transduced cells from host mice given i.v. co-transfer of P14 $CD8^+$ that had been activated *in vitro* and transduced for 6h with shControl or shYBX1, followed by i.p. infection of the recipients with LCMV Armstrong (as in **3A**). Splenocytes were analyzed 30 days later for CD62L and IL-7R expression. Numbers in quadrants indicate percent cells. Plot on the right indicates gating strategy for LLE, T_{EM} and T_{CM} subsets. **(B)** Quantification of splenic LLE, T_{EM}, and T_{CM} $CD8^+$ T cells as in **A**. **(C)** Frequency of splenic LLE (left), T_{EM} (middle), and T_{CM} (right) $CD8^+$ T cells as in **A**. **(D)** Flow cytometry of splenocytes was performed 30 days after infection as described in **A** and analysis of TNF-α, IFN-γ, and IL-2 expression is shown. Cells were stimulated for 4 hours with gp33 peptide. Numbers in quadrants indicate percent cells. **(E)** Quantification (left) or frequency (right) of splenic TNF-α^+ IFN-γ^+ $CD8^+$ T cells as in **D. (F)** Quantification (left) or frequency (right) of splenic IL-2^+ $CD8^+$ T cells as in **D. (G)** MFI of splenic TNF-α^+ (left), IFN-γ^+ (middle), or IL-2^+ (right) $CD8^+$ T cells as in **D**. **(H)** Flow cytometry of cells as described in **A**. IEL isolated from the small intestinal tissue were analyzed 30 days later and CD69 and CD103 expression was quantified. Numbers in quadrants indicate percent cells. **(I)** Quantification (left) or frequency (right) of IEL $CD8^+$ $CD69^+$ $CD103^+$ cells as in **H**. n = 5 for all groups. Data reported as mean +/- SEM. * $P < .05$, ** $P < .01$ (paired parametric t-test). Data are representative of four experiments.

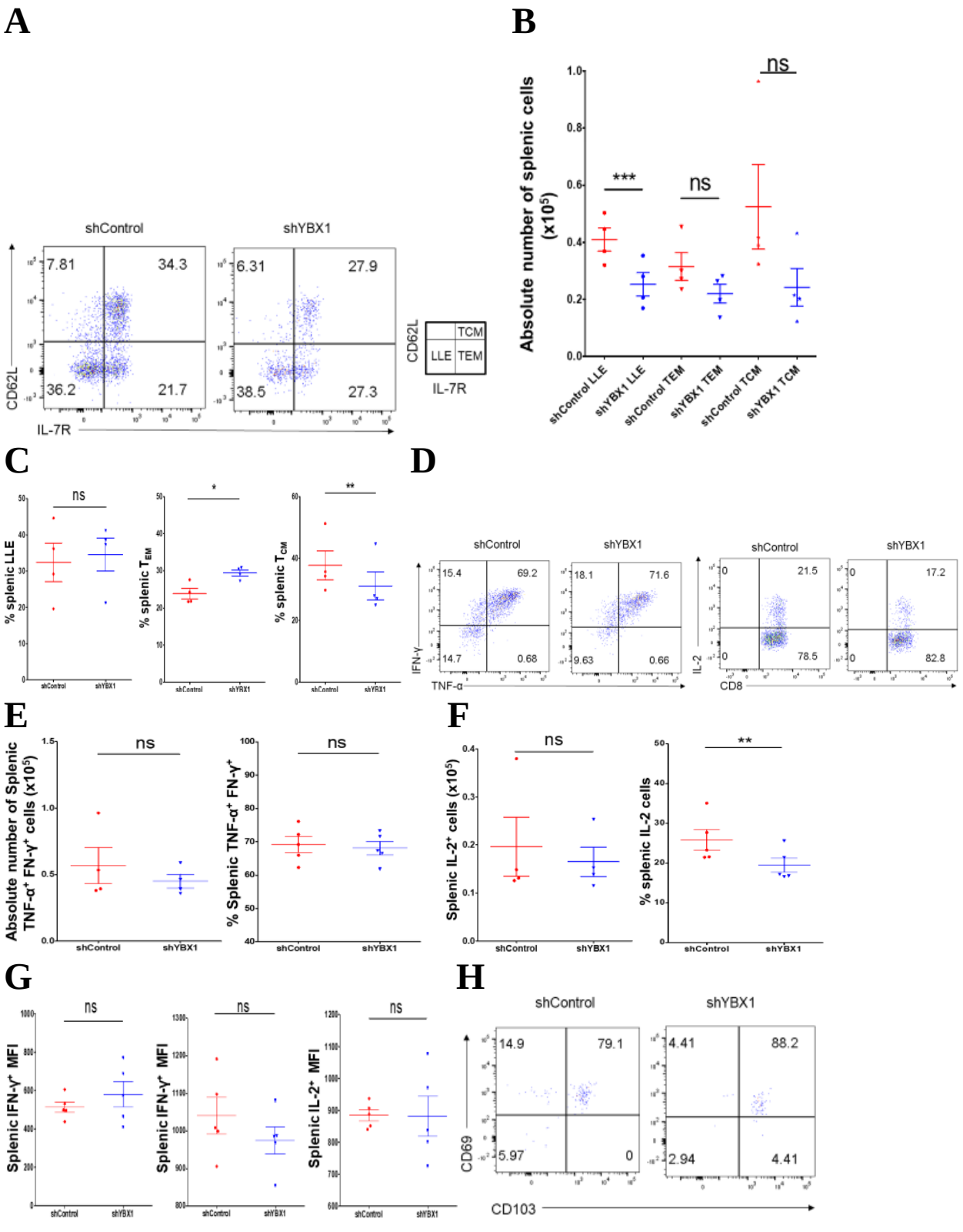
A
shControl
shYBX1
7.81
34.3
36.2
21.7
6.31
27.9
38.5
27.3
CD62L
IL-7R
LLE
TCM
TEM
B
Absolute number of splenic cells (x10^5)
***
ns
ns
shControl LLE
shYBX1 LLE
shControl TEM
shYBX1 TEM
shControl TCM
shYBX1 TCM
C
% splenic LLE
% splenic T_EM
% splenic T_CM
D
IFN-γ
TNF-α
IL-2
CD8
E
Absolute number of Splenic TNF-α+ FN-γ+ cells (x10^5)
% Splenic TNF-α+ FN-γ+
F
Splenic IL-2+ cells (x10^5)
% splenic IL-2 cells
G
Splenic IFN-γ+ MFI
Splenic IL-2+ MFI
H
CD69
CD103
14.9
79.1
5.97
0
4.41
88.2
2.94
4.41

Figure 5 continued.

I

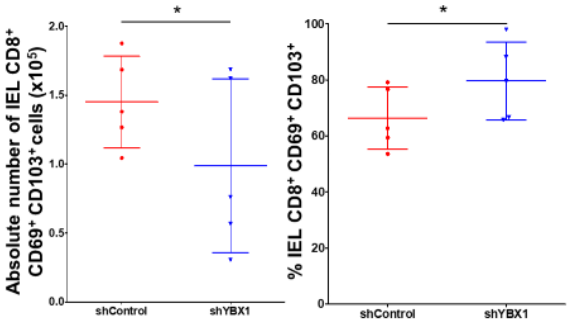

Discussion

The cold shock domain proteins YBX1 and YBX3 are known to play roles in cell trafficking, inflammatory responses, cytokine production, and cellular proliferation in cancer models (Brandt et al., 2012), but whether YBX1 and YBX3 play roles in $CD8^+$ T cell differentiation and function during viral infection has not yet been investigated. Here, we used an shRNA-based knockdown approach to study the roles of YBX1 and YBX3 in $CD8^+$ T cell differentiation in response to acute viral infection. We show that YBX1 and YBX3 regulate differentiation of TE cells, circulating T_{CM} and T_{EM} cells, and small intestine T_{RM} cells. Functionally, we also show that YBX1 and YBX3 regulate the production of the cytokines IFN-γ, TNF-α, and IL-2 in both circulating and tissue-resident $CD8^+$ T cells. Taken together, these data suggest that YBX1 and YBX3 play previously unappreciated roles in $CD8^+$ T cell differentiation and function.

YBX1 and YBX3 appear to share overlapping functions, as similar effects were observed when each was knocked down in $CD8^+$ T cells responding to acute infection. When YBX1 and YBX3 were knocked down, we observed decreased frequency and number of $CD8^+$ TE ($KLRG1^{hi}IL\text{-}7R^{lo}$) cells seven days after infection and decreased frequency of $CD8^+$ T_{CM} ($CD62L^{hi}IL\text{-}7R^{hi}$) cells 30 days after infection. Additionally, when YBX1 and YBX3 were knocked down, $CD8^+$ MP ($KLRG1^{hi}IL\text{-}7R^{hi}$) cells, and $CD8^+$ $CD69^+$ $CD103^+$ cells found within the small intestine were increased in frequency seven days after infection. Knockdown of YBX1 or YBX3 resulted in increased frequencies of $CD8^+$ T_{EM} ($CD62L^{lo}IL\text{-}7R^{hi}$) cells and small intestine $CD8^+$ T_{RM} cells 30 days post-infection. Our data showed significant increases in $CD8^+$ T cell production of IFN-γ, TNF-α, and IL-2, which suggests a role for the YBX genes role in regulating of $CD8^+$ T cell function.

Both YBX1 and YBX3 are cold shock domain proteins that exert pleiotropic functions in cells as transcriptional and translational regulators (Jady B., Ketele A., Kiss T., 2018, Kohno K., Izumi H., Uchiumi T., Ashizuka M., Kuwano M., 2003, Lindquist et al. 2014, Suresh P., Tsutusmi R., Venkatesh T., 2018). YBX1 has been shown to be an extracellular mitogen and regulates DNA polymerase α expression controlling DNA replication and cellular proliferation (Fyre et al., 2009, En-Nia et al., 2004, Leveonson V., Davidovich I., Roninson I., 2000, Ladomery M., and Sommerville J., 1995). There have been few published studies on YBX3; cancer studies have reported that overexpression of YBX3 results in inhibited tumor growth and reduced density of lymphatic vessels within primary tumors *in vivo*. Moreover, it has been shown that YBX3 expression is down-regulated in breast cancer compared to healthy tissue (Matsumoto G. et al., 2010, Saito Y. et al., 2008, Hu Y. et al., 2004). Our data indicated that both YBX1 and YBX3 regulate proliferation in $CD8^+$ T cells. When expression of YBX3 is reduced, the number of cells is increased relative to control cells; the opposite is true for YBX1, suggesting that both YBX1 and YBX3 expression can impact cellular proliferation. Furthermore, we observed that inhibition of YBX3 expression resulted in increased levels of IL-2 production. These observations are in line with studies demonstrating regulation of IL-2 translation in T cells when YBX1 mRNA expression is increased (Chen C. et al., 2000, Seko Y., Cole S., Kasprzak W., Shapiro B., Ragheb J., 2005) and demonstrate that YBX3 also plays an important role in regulation of cytokine production in $CD8^+$ T cells.

In conclusion, we show that YBX1 and YBX3 are important for regulating $CD8^+$ T cell differentiation. Reducing the expression of YBX1 and YBX3 in activated $CD8^+$ T cells during acute infection resulted in a significant decrease in the frequencies of $CD8^+$ TE cells and $CD8^+$ T_{CM} cells. Knockdown of YBX1 and YBX3 resulted in increased frequencies of circulating

$CD8^+$ MP and T_{EM} cells, as well as small intestine $CD8^+$ T_{RM} cells. YBX1 and YBX3 both play a role in $CD8^+$ T cell function as knockdown of YBX1 or YBX3 caused increased frequencies of IFN-γ, TNF-α, and IL-2 producing $CD8^+$ T cells. Further studies will be to investigate the mechanisms by which YBX1 and YBX3 interact and regulate T cell differentiation and function.

References

Badovinac, Vladimir P., Brandon B. Porter, and John T. Harty. "CD8 T Cell Contraction Is Controlled by Early Inflammation." *Nature Immunology* 5, no. 8 (2004): 809-17. doi:10.1038/ni1098.

Bender, B. S., Croghan T., Zhang L., Small P., "Transgenic Mice Lacking Class I Major Histocompatibility Complex- Restricted T Cells Have Delayed Viral Clearance and Increased Mortality after Influenza Virus Challenge." *Journal of Experimental Medicine* 175, no. 4 (1992): 1143-145. doi:10.1084/jem.175.4.1143.

Bergmann, Stephan, Brigitte Royer-Pokora, Ellen Fietze, Karsten Jürchott, Barbara Hildebrandt, Detlef Trost, Frauke Leenders, Jenny-Chang Claude, Franz Theuring, Ralf Bargou, Manfred Dietel, and Hans-Dieter Royer. "YB-1 Provokes Breast Cancer through the Induction of Chromosomal Instability That Emerges from Mitotic Failure and Centrosome Amplification." *Cancer Research* 65, no. 10 (2005): 4078-087. doi:10.1158/0008-5472.can-04-4056.

Bernhardt, Anja, Alexander Fehr, Sabine Brandt, Saskia Jerchel, Tobias M. Ballhause, Lars Philipsen, Saskia Stolze, Robert Geffers, Honglei Weng, Klaus-Dieter Fischer, Berend Isermann, Monika C. Brunner-Weinzierl, Arvind Batra, Britta Siegmund, Cheng Zhu, Jonathan A. Lindquist, and Peter R. Mertens. "Inflammatory Cell Infiltration and Resolution Of kidney Inflammation Is Orchestrated by the Cold-shock Protein Y-box Binding Protein-1." *Kidney International*92, no. 5 (2017): 1157-177. doi:10.1016/j.kint.2017.03.035.

Brandt, Sabine, Ute Raffetseder, Sonja Djudjaj, Anja Schreiter, Bert Kadereit, Melanie Michele, Melanie Pabst, Cheng Zhu, and Peter R. Mertens. "Cold Shock Y-box Protein-1 Participates in Signaling Circuits with Auto-regulatory Activities." *European Journal of Cell Biology* 91, no. 6-7 (2012): 464-71. doi:10.1016/j.ejcb.2011.07.002.

Chang, John T., E. John Wherry, and Ananda W. Goldrath. "Molecular Regulation of Effector and Memory T Cell Differentiation." *Nature Immunology* 15, no. 12 (2014): 1104-115. doi:10.1038/ni.3031.

Chen, Ching-Yi, Roberto Gherzi, Jens S. Andersen, Guido Gaietta, Karsten Jürchott, Hans-Dieter Royer, Matthias Mann, and Michael Karin. "Nucleolin and YB-1 Are Required for JNK-mediated Interleukin-2 MRNA Stabilization during T-cell Activation." *Genes Dev.* 14:1236-248. doi:10.1101/gad.14.10.1236.

En-Nia, Abdelaziz, Emek Yilmaz, Uwe Klinge, David H. Lovett, Ioannis Stefanidis, and Peter R. Mertens. "Transcription Factor YB-1 Mediates DNA Polymerase α Gene Expression." *Journal of Biological Chemistry* 280, no. 9 (2004): 7702-711. doi:10.1074/jbc.m413353200

Faassen, H. Van, M. Saldanha, D. Gilbertson, R. Dudani, L. Krishnan, and S. Sad. "Reducing the Stimulation of CD8 T Cells during Infection with Intracellular Bacteria Promotes Differentiation Primarily into a Central (CD62LhighCD44high) Subset." *The Journal of Immunology* 174, no. 9 (2005): 5341-350. doi:10.4049/jimmunol.174.9.5341.

Frye, Björn C., Sarah Halfter, Sonja Djudjaj, Philipp Muehlenberg, Susanne Weber, Ute Raffetseder, Abdelaziz En-Nia, Hanna Knott, Jens M. Baron, Steven Dooley, Jürgen Bernhagen, and Peter R. Mertens. "Y-box Protein-1 Is Actively Secreted through a Non-classical Pathway and Acts as an Extracellular Mitogen." *EMBO Reports* 10, no. 7 (2009): 783-89. doi:10.1038/embor.2009.81.

Gerlach, Carmen, Jeroen W.j. Van Heijst, Erwin Swart, Daoud Sie, Nicola Armstrong, Ron M. Kerkhoven, Dietmar Zehn, Michael J. Bevan, Koen Schepers, and Ton N.m. Schumacher. "One Naive T Cell, Multiple Fates in CD8 T Cell Differentiation." *The Journal of Experimental Medicine* 207, no. 6 (2010): 1235-246. doi:10.1084/jem.20091175.

Hamann, D., P. A. Baars, M. H.g. Rep, B. Hooibrink, S. R. Kerkhof-Garde, M. R. Klein, and R. A.w. V. Lier. "Phenotypic and Functional Separation of Memory and Effector Human CD8 T Cells." *Journal of Experimental Medicine* 186, no. 9 (1997): 1407-418. doi:10.1084/jem.186.9.1407.

Harty, John T., and Vladimir P. Badovinac. "Shaping and Reshaping CD8 T-cell Memory." *Nature Reviews Immunology* 8, no. 2 (2008): 107-19. doi:10.1038/nri2251.

Hu, Yuhui, Hongxia Sun, Jeffrey Drake, Frances Kittrell, Martin C. Abba, Li Deng, Sally Gaddis, Aysegul Sahin, Keith Baggerly, Daniel Medina, and C. Marcelo Aldaz. "From Mice to Humans." *Cancer Research* 64, no. 21 (2004): 7748-755. doi:10.1158/0008-5472.can-04-1827.

Huster, K. M., V. Busch, M. Schiemann, K. Linkemann, K. M. Kerksiek, H. Wagner, and D. H. Busch. "Selective Expression of IL-7 Receptor on Memory T Cells Identifies Early CD40L-dependent Generation of Distinct CD8 Memory T Cell Subsets." *Proceedings of the National Academy of Sciences*101, no. 15 (2004): 5610-615. doi:10.1073/pnas.0308054101.

Joshi, Nikhil S., Weiguo Cui, Anmol Chandele, Heung Kyu Lee, David R. Urso, James Hagman, Laurent Gapin, and Susan M. Kaech. "Inflammation Directs Memory Precursor and Short-Lived Effector CD8 T Cell Fates via the Graded Expression of T-bet Transcription Factor." *Immunity* 27, no. 2 (2007): 281-95. doi:10.1016/j.immuni.2007.07.010.

Jády, Beáta E., Amandine Ketele, and Tamás Kiss. "Dynamic Association of Human MRNP Proteins with Mitochondrial TRNAs in the Cytosol." *Rna*24, no. 12 (2018): 1706-720. doi:10.1261/rna.066738.118.

Kaech, Susan M., Joyce T. Tan, E. John Wherry, Bogumila T. Konieczny, Charles D. Surh, and Rafi Ahmed. "Selective Expression of the Interleukin 7 Receptor Identifies Effector CD8 T Cells That Give Rise to Long-lived Memory Cells." *Nature Immunology* 4, no. 12 (2003): 1191-198. doi:10.1038/ni1009.

Kaech Susan M., and E. John Wherry. "Heterogeneity and Cell-Fate Decisions in Effector and Memory CD8 T Cell Differentiation during Viral Infection." *Immunity* 27, no. 3 (2007): 393-405. doi:10.1016/j.immuni.2007.08.007.

Kakaradov, Boyko, Janilyn Arsenio, Christella E. Widjaja, Zhaoren He, Stefan Aigner, Patrick J. Metz, Bingfei Yu, Ellen J. Wehrens, Justine Lopez, Stephanie H. Kim, Elina I. Zuniga, Ananda W. Goldrath, John T. Chang, and Gene W. Yeo. "Early Transcriptional and Epigenetic Regulation of CD8 T Cell Differentiation Revealed by Single-cell RNA Sequencing." *Nature Immunology* 18, no. 4 (2017): 422-32. doi:10.1038/ni.3688.

Kohno, Kimitoshi, Hiroto Izumi, Takeshi Uchiumi, Megumi Ashizuka, and Michihiko Kuwano. "The Pleiotropic Functions of the Y-box-binding Protein, YB-1." *BioEssays* 25, no. 7 (2003): 691-98. doi:10.1002/bies.10300.

Kumar, Brahma V., Wenji Ma, Michelle Miron, Tomer Granot, Rebecca Guyer, Dustin Carpener, Takashi Senda, Xiaoyun Sun, Siu-Hong Ho, Harvey Lerner, Amy Friedman, Yufeng Shen, and Donna Farber. "Human Tissue-Resident Memory T Cells Are Defined by Core Transcriptional and Functional Signatures in Lymphoid and Mucosal Sites." *SSRN Electronic Journal*, 2018. doi:10.2139/ssrn.3155546.

Ladomery, Michael, and John Sommerville. "A Role for Y-box Proteins in Cell Proliferation." *BioEssays*17, no. 1 (1995): 9-11. doi:10.1002/bies.950170104.

Leveonson (Chernokhvostov), Victor V., Irina A. Davidovich, and Igor B. Roninson. "Pleiotropic Resistance to DNA-interactive Drugs Is Associated with Increased Expression of Genes Involved in DNA Replication, Repair, and Stress Response." *Cancer Research* 60, no. 18 (September 2000). http://cancerres.aacrjournals.org/content/60/18/5027.

Lindquist, Jonathan A., Sabine Brandt, Anja Bernhardt, Cheng Zhu, and Peter R. Mertens. "The Role of Cold Shock Domain Proteins in Inflammatory Diseases." *Journal of Molecular Medicine* 92, no. 3 (2014): 207-16. doi:10.1007/s00109-014-1136-3.

Lovett, David H., Sunfa Cheng, Leslie Cape, Allan S. Pollock, and Peter R. Mertens. "YB-1 Alters MT1-MMP Trafficking and Stimulates MCF-7 Breast Tumor Invasion and Metastasis." *Biochemical and Biophysical Research Communications* 398, no. 3 (2010): 482-88. doi:10.1016/j.bbrc.2010.06.104.

Matsumoto, Goichi, Nobuyuki Yajima, Hiroyuki Saito, Hironori Nakagami, Yasushi Omi, Ushaku Lee, and Yasufumi Kaneda. "Cold Shock Domain Protein A (CSDA) Overexpression Inhibits Tumor Growth and Lymph Node Metastasis in a Mouse Model of Squamous Cell Carcinoma." *Clinical & Experimental Metastasis* 27, no. 7 (2010): 539-47. doi:10.1007/s10585-010-9343-y.

Saito, Y., H. Nakagami, M. Kurooka, Y. Takami, Y. Kikuchi, H. Hayashi, T. Nishikawa, K. Tamai, R. Morishita, N. Azuma, T. Sasajima, and Y. Kaneda. "Cold Shock Domain Protein A Represses Angiogenesis and Lymphangiogenesis via Inhibition of Serum Response Element." *Oncogene* 27, no. 13 (2007): 1821-833. doi:10.1038/sj.onc.1210824.

Sallusto, Federica, Danielle Lenig, Reinhold Förster, Martin Lipp, and Antonio Lanzavecchia. "Two Subsets of Memory T Lymphocytes with Distinct Homing Potentials and Effector Functions." *Nature* 401, no. 6754 (1999): 708-12. doi:10.1038/44385.

Sathaliyawala, Taheri, Masaru Kubota, Naomi Yudanin, Damian Turner, Philip Camp, Joseph J.c. Thome, Kara L. Bickham, Harvey Lerner, Michael Goldstein, Megan Sykes, Tomoaki Kato, and Donna L. Farber. "Distribution and Compartmentalization of Human Circulating and Tissue-Resident Memory T Cell Subsets." *Immunity* 38, no. 1 (2013): 187-97. doi:10.1016/j.immuni.2012.09.020.

Schenkel, Jason M., and David Masopust. "Tissue-Resident Memory T Cells." *Immunity* 41, no. 6 (2014): 886-97. doi:10.1016/j.immuni.2014.12.007.

Seder, Robert A., Patricia A. Darrah, and Mario Roederer. "T-cell Quality in Memory and Protection: Implications for Vaccine Design." *Nature Reviews Immunology*8, no. 4 (2008): 247-58. doi:10.1038/nri2274.

Seko, Yuko, Steven Cole, Wojciech Kasprzak, Bruce A. Shapiro, and Jack A. Ragheb. "The Role of Cytokine MRNA Stability in the Pathogenesis of Autoimmune Disease." *Autoimmunity Reviews*5, no. 5 (2006): 299-305. doi:10.1016/j.autrev.2005.10.013.

Sheridan, Brian S., and Leo Lefrançois. “Intraepithelial Lymphocytes: To Serve and Protect.” *Current Gastroenterology Reports*, vol. 12, no. 6, 2010, pp. 513–521., doi:10.1007/s11894-010-0148-6.

Suresh, Padmanaban S., Rie Tsutsumi, and Thejaswini Venkatesh. "YBX1 at the Crossroads of Non-coding Transcriptome, Exosomal, and Cytoplasmic Granular Signaling." *European Journal of Cell Biology*97, no. 3 (2018): 163-67. doi:10.1016/j.ejcb.2018.02.003.